A Complete DC Trolleybus Grid Model With Bilateral Connections, Feeder Cables, and Bus Auxiliaries

Diab, Ibrahim; Saffirio, Alice ; Mouli, Gautham Ram Chandra; Tomar, Abhishek Singh; Bauer, Pavol

DOI
10.1109/TITS.2022.3157080

Publication date
2022

Document Version
Final published version

Published in
IEEE Transactions on Intelligent Transportation Systems

A Complete DC Trolleybus Grid Model With Bilateral Connections, Feeder Cables, and Bus Auxiliaries

Ibrahim Diab, *Student Member, IEEE*, Alice Saffirio, Gautham Ram Chandra Mouli, *Member, IEEE*, Abhishek Singh Tomar, and Pavol Bauer, *Senior Member, IEEE*

***Abstract*— This paper offers a complete and verified model of DC trolleybus grids and examines the effect of the common modelling assumptions made in literature by using simulations, as well as bus and substation measurements from the grid of Arnhem, the Netherlands. An equivalent model for the overhead line impedance is offered taking into account the single line impedance, the supply and return lines, and the parallel connections between them. A case study shows that the feeder cables from the substations to the sections can be ignored, but only for certain substation power and feeder-line length ranges. On the other hand, the often-neglected regenerative braking, bus auxiliaries load, bilateral connections, and the exact nominal substation voltage are found to be crucial for the correct modelling of a trolleybus grid.**

***Index Terms*— DC power systems, electrical transportation, public transport, regenerative braking, trolleybus.**

ABBREVIATIONS

BN	Bilateral Node.
FC	Feeder Cable.
HVAC	Heating, Ventilation, and Air Conditioning.
LVAC	Low Voltage AC grid.
SN	Slack Node.

NOMENCLATURE

α	Section average power loss percentage [%].
ΔV_{f}	Voltage drop across the feeder cable [V].
ΔV_{tr}	Voltage drop between the substation and the bus [V].
λ	Overhead line inductance per meter [H/m].
ρ	Overhead line resistance per meter [Ω/m].
i	Current drawn by the bus [A].
I_{SN}	Slack node current [A].
i_{s}	Substation current [A].
l_{b}	Total distance bus-substation [m].
l_{lp}	Distance between parallel-line connections [m].
l_{p}	Highest multiple integer of l_{lp} below l_{b} [m].
l_{s}	Single segment length [m].
P_{aux}	Bus auxiliaries power [kW].
P_{base}	Bus base loads power [kW].
P_{BN}	Power of bilateral node [kW].
P_{BR}	Bus power wasted in the braking resistor [kW].
P_{bus}	Bus power [kW].
P_{net}	Bus net power exchanged with the grid [kW].
P_{rated}	HVAC nominal power [kW].
P_{tr}	Bus traction power [kW].
$P_{\mathrm{loss},f}$	Power lost in the feeder cable [kW].
Q_{c}	Conductive and convective heat transfer load [kWh].
Q_{d}	Heat exchange from bus doors opening [kWh].
Q_{m}	The metabolic heat from passenger bodies [kWh].
Q_{s}	Solar heat gain due to solar radiation [kWh].
Q_{v}	Heat exchange due to the forced air ventilation [kWh].
R_{f}	Impedance of the feeder cable [Ω].
$R_{n,n-1}$	Impedance between nodes n and n-1 [Ω].
t_{cycle}	HVAC duty cycle period [s].
t_{on}	HVAC on time in one cycle [s].
V_{BN}	Voltage of bilateral node [V].
V_{ss2}	Bilateral substation nominal voltage [V].
v_{bus}	Bus velocity [m/s].
V_{c}	Voltage at the substation-section connection [V].
V_{ds}	Voltage blocked by substation rectifiers [V].
V_{fd}	Voltage drop across feeding or return line [V].
x_{bus}	Bus distance from the substation [m].

Manuscript received 3 August 2021; revised 11 January 2022; accepted 28 February 2022. Date of publication 16 March 2022; date of current version 11 October 2022. This work was supported by the Trolley 2.0 Project, under Electric Mobility Europe. The Associate Editor for this article was T. Q. Dinh. *(Corresponding author: Ibrahim Diab.)*

Ibrahim Diab, Alice Saffirio, Gautham Ram Chandra Mouli, and Pavol Bauer are with the Electrical Sustainable Energy Department, TU Delft, 2628 Delft, The Netherlands (e-mail: i.diab@tudelft.nl).

Abhishek Singh Tomar is with HAN Automotive Research, HAN University of Applied Sciences, 6802 Arnhem, The Netherlands.

Digital Object Identifier 10.1109/TITS.2022.3157080

I. INTRODUCTION

THE trolleybus is an electric bus that is supplied by overhead lines (catenary), similar to the way a tram operates. Changing attitudes toward diesel buses is bringing trolleybuses back into the transportation landscape as a key player in transportation electrification [1]. Trolleybuses consume about 70 kW during regular driving, and can reach demands higher than 300 kW while accelerating. When a trolleybus brakes, the available regenerative braking power can be as high as 200 kW. While some solutions exist, for example with on-board storage devices [2], this available energy,

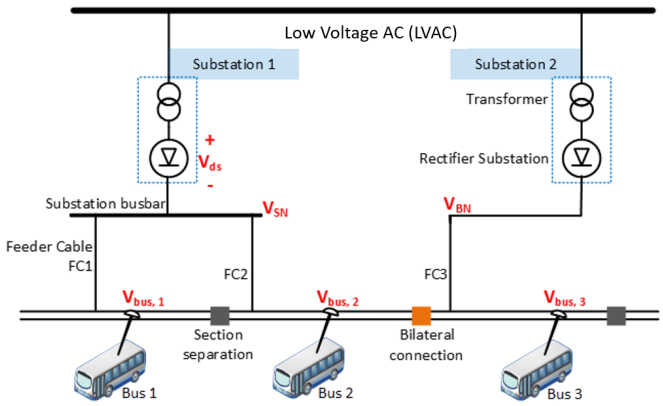

Fig. 1. The trolleygrid and its components.

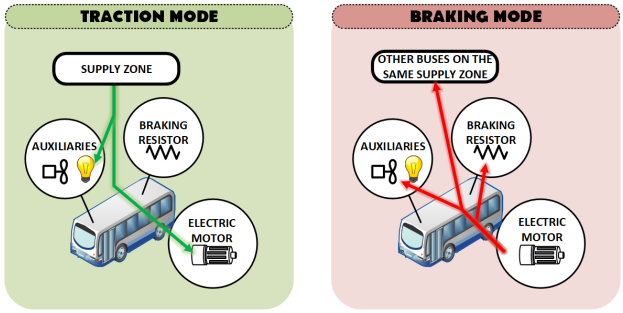

Fig. 2. The bus power flow: In traction mode, the power from the supply zone (substation(s) and/or regenerating bus(es)) feeds the motor and auxiliaries. In braking mode, the power is used to supply the auxiliaries and any other bus on the same supply zone. Excess energy is wasted in the braking resistor.

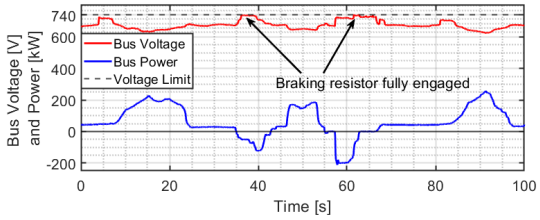

Fig. 3. Bus voltage and power measurements from the trolleygrid in Arnhem, the Netherlands. The braking resistor is fully engaged when the generating bus voltage rises to the upper voltage limit of the grid (740V in Arnhem).

is frequently wasted in on-board braking resistors, as will be discussed later.

Figure 1 shows the typical layout of a trolleygrid. For reasons such as faults and transmission losses, the trolleybus lines are divided into isolated sections of few hundreds of meters, up to 1 or 2 km, depending on the trolleygrid city. The power comes from the Low Voltage AC grid (Low Voltage AC grid (LVAC)) and a transformer steps down the voltage, then a rectifier converts into to DC, as the buses run at a nominal voltage of 600-700V. The minimum voltage, due to transmission voltage drops, that the bus runs on is 400V. The transformer-rectifier system is housed in a "substation". One substation can feed one or more sections, to which it is connected via the section feeder cables (Feeder Cable (FC)). In figure 1, substation 1 feeds two sections, while substation 2 feeds one.

The substations are unidirectional because of the rectifier. Consequently, a braking bus cannot send its energy back to the LVAC grid, but rather to other buses on the same section, or on a connected section. The first possibility for two sections to be connected is when they are supplied by the same substation: Bus 1 of figure 1, for example, can supply Bus 2 via the route FC1-substation busbar-FC2. The second possibility is when the sections are bilaterally connected. A bilateral connection is a controllable connection between two sections that are under different substations. The connection can be controlled as closed (connected) or open (isolated). Bus 2 can send power through the overhead lines to bus 3 as if sections 2 and 3 are one long section. Bus 1 can also share power with bus 3 via the route FC1-busbar-FC2-bilateral.

Finally, it is noticeable that each bus is connected to two lines in figure 1. In trolleygrids, an overhead return path for the current is also needed as the bus runs on wheels, unlike the tram which uses the rails as a return. In this paper, we define "supply zone" as the electrically connected zone in which a bus can send and receive power. Thanks to the bilateral connection, all the elements shown in figure 1 are part of one supply zone. The bus is supplied with the power to feed its traction and non-traction demands (figure 2). When a bus is braking, in the absence of a receiving bus on the same supply zone or if the braking energy is excessive, the excess braking energy is wasted on-board in the braking resistors. The amount of energy wasted is controlled by a chopper circuit that controls the on-time of the resistors as to keep the grid voltage below the allowable upper limit (around 780V, depending on the city). At values of around 720-740V, also depending on the trolleygrid, the braking resistor is fully engaged to prevent any over-voltages (see figure 3).

To reduce the transmission losses on the section, an element found commonly in transport networks is the parallel connection between the overhead lines of the different bus lines available in a section; i.e, the going and the returning traffic lines. Within the same section, the feed (positive) and the return (negative) lines are connected in pairs to offer a lower impedance path from the substation (or a braking bus) to the buses. These lines are introduced periodically at a distance in the order of hundreds of meters (100-300m). This paper looks at Arnhem, the Netherlands, as a case study. In Arnhem, for example, these parallel lines are currently being changed from a frequency of 150m to one of 100m.

A. Modelling of Trolleygrids in Literature

Modelling transportation networks has been a powerful tool in designing, analyzing, and optimizing electrical transit grids. Simulators, both commercial and academic [3]–[28], use different solver methods and modelling techniques to investigate these networks. Generally, these simulators are used to calculate substation-level parameters such as the substation power demand and the substation components design rating.

Nevertheless, many studies look more in depth into variables such as the voltage drops over the transmission lines for the introduction of larger buses on the lines, for example, or the available braking energy for recuperation by storage devices.

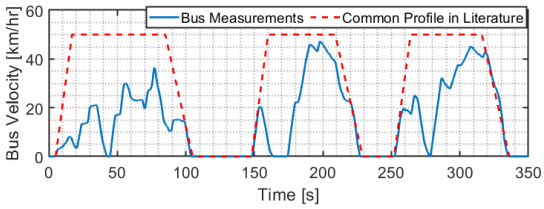

Fig. 4. Bus velocity measurements in Arnhem compared to the trapezoidal velocity profile commonly found in literature. The latter assumes a constant acceleration phase from the bus stop, followed by a constant-velocity cruising at 50 km/hr, and then a constant deceleration toward the next bus stop.

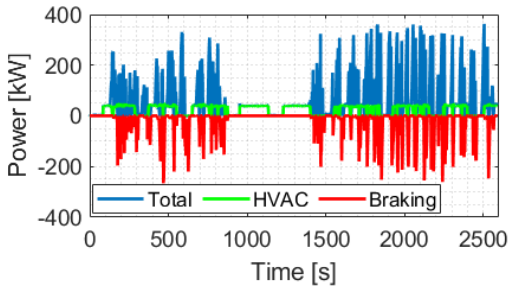

Fig. 5. Total, HVAC, and braking bus power measurements for an exemplary drive on trolleybus line 1 in Arnhem, the Netherlands on 22 January 2019.

Unfortunately, these models are limited both in the modelling of the bus load and of the grid elements. Trolleygrid studies tend to limit themselves to a single section, with an ideal trapezoidal traction power load [3], [4], [12], [15], [16], [23], [24]. A trapezoidal profile assumes a constant acceleration phase from the bus stop, followed by a constant-velocity cruising at 50 km/hr, and then a deceleration toward the next bus stop. As figure 4 shows, this is not a fair representation of the actual velocity profile of the trolleybuses. The traffic conditions can seriously affect the bus consumption as explained in [29].

While some sources use a more sophisticated bus traction power model [9], [13], [19], [27], they still neglect the seasonal variation of the bus demand brought by the auxiliaries, namely the HVAC (heating, ventilation, and air conditioning) [3]–[5], [9], [12], [15], [16], [19], [23], [24]. During winter conditions, this demand can be as high as the traction load (about 1.5 kWh/km each) as measurements have shown in figure 5 where the total HVAC demand of 17.95kWh accounts for half of the bus total demand of 36.11 kWh during the 11.60 km trip. This value is in accordance with those previously reported in literature [30], [31]. Ignoring this HVAC power would have two consequences. First, it would remove a considerable portion of the substation load, making substation calculation inaccurate. Second, it removes a receiver of the bus regenerative braking (see figure 2) which would result in inaccurate calculations of the shared energy between buses and of the energy wasted in the on-board braking resistors. This underestimates the substation demand brought by lower loads, and higher power sharing between buses. The regenerative braking can also feed other buses that are under the same supply zone, relieving the two bilaterally connected substations from a fraction of the bus load. Measurements made on the trolleybuses in Arnhem (figure 5) have shown that around 30% of the bus load is available for recuperation (12.00 of the 36.11kWh). This value is in line with what is reported in other trolley cities [2], [3], [10], [14]. Without a bilateral connection correctly modelled, this available energy would be assumed wasted in the on-board braking resistors, and causing an overestimation of the substation energy demand. Finally, the feeder cables can affect the regenerative braking and the bilateral connection by contributing to a sizeable voltage drop on the section, altering the supplied power share by the substations and the braking buses. This can happen when the voltage of one node, for example, becomes too low relative to the other supplying nodes, and is therefore unable to push power into the circuit.

Other than the simplistic bus models, the trolleygrid itself is frequently modelled with some major assumptions. For example, some works consider the parallel lines ([5], [7], [26]) while others, such as [4], [8], ignore them. Feeder cables are also ignored, except in few works ([18], [20], [26]).

The need for a complete bus power representation and trolleygrid model is more pressing nowadays. This is because DC trolleygrids are ushering a new era of active, urban transportation grids as they look at integrating solar PV [15], [16], on-board and/or off-board storage [4], [17], [22], [27], electric-vehicle (EV) chargers [15], [32], [33], and In-Motion-Charging (IMC) buses [34], [35] into their network. To highlight an example of the future grid, IMC buses are the new generation of trolleys that combine the advantage of a catenary operation, with the flexibility of an electric battery-bus. The IMC bus is equipped with a battery that is charged while the bus is under the catenary (the charging corridor), and discharged later when the trolleybus is driving in areas outside the trolleygrid. The main urban advantages of such a system can be, for example, in operating these buses in historic city centers without the visual intrusion of lines, or in operating over new lines without the need for building a new infrastructure. With a battery charging at the order of hundreds of kWs, these buses constitute a challenge in the expansion of the trolleygrid. A detailed model for the power consumption and the voltage drop at the substation level is needed to make sure that the introduction of IMC does not violate the operational limits. As sections III-E and III-F show, respectively, the simplified grid models found in literature can lead to incorrect results in the calculation of the minimum voltage and of load demand on a substation.

It is then particularly important for this subgroup of transportation grids to study in detail the line voltage, current ratings, and the in-line transmission losses of their subsystems, using specific, representative models.

In particular, seven parameters that are often ignored and/or approximated in these models are:

- The inductive component of the overhead line impedance,
- The parallel lines connecting the overhead lines,
- The bus auxiliaries power (predominately the HVAC),
- The bus regenerative braking,
- The section feeder cables,
- The bilateral connections between sections,
- The nominal voltage of the substation

TABLE I
SUMMARY OF THE COMPARISON BETWEEN COMMON ASSUMPTIONS IN LITERATURE AND THE TROLLEYBUS MODEL IN THIS PAPER

Trolleygrid Parameter	Typical Modelling Assumptions Made in Literature	Effect of Assumption (case study analysis in this paper)	Detailed Explanation
Overhead Line Impedance	Assumed purely resistive, expect in works such as [17] where it is taken as resistive-inductive	Can indeed be considered purely resistive for steady-state models	section III-A
Overhead Parallel Lines	Ignored in works such as [4], [8], included in works such as [5], [7], [26]	If ignored, the line impedance could be as much as double its actual value (100% error)	section III-B
Bus Auxiliaries Power	Ignored in works such as [3]–[5], [9], [12], [15], [16], [19], [23], [24], included in works such as [6], [14]	If ignored, errors up to 55% in substation energy calculations	section III-C
Bus Regenerative Braking	Ideally, implied that it is modelled but it is not correct to include it while simultaneously ignoring the auxiliaries demand such as in [3]–[5], [9], [12], [15], [16], [19], [23], [24]	If ignored, errors as high as 34% in the substation power calculations	section III-D
Section Feeder Cable	Only mentioned in works such as [18], [20], [26]	If ignored, errors are expected in extreme cases above 15% in the substation power calculations and 50V for the minimum line voltage. However, equations 19 and 20 offer an easy way to estimate where these cables can still be ignored	section III-E
Bilateral Connections	Only mentioned in works such as [7], [25], [36]	If ignored, errors up to 25% in the substation power calculations	section III-F
Substation Nominal Voltage	Typically assumed at a rounded-up nominal value of 650 or 700V such as in [4], [36], [37]	Particularly important for bilaterally connected substations because of the effect on the load-sharing ratio between them	section III-G

In brief, the study of the future trolleygrid requires more specific models with proper representation of the bus load and grid elements. While many works in literature include some of these elements, to the knowledge of the authors, no work has included all of them as presented in this paper. The effects and errors from excluding these elements is also studied in this work and summarized in Table I.

B. Paper Contributions

This paper offers the following 3 contributions:

1) A complete and experimentally verified trolleybus grid model that includes typically overlooked elements of the system, and that can be used for unilateral and bilateral substations. A new modelling method for bilaterally connected substations as an equivalent stationary regenerating bus is also offered
2) An equivalent-impedance model for the overhead lines taking into account the line impedance and parallel connections between the lines
3) A quantification of the effect of the non-traction component of the bus power profile (regenerative braking and auxiliaries) and of the trolleygrid architecture (feeder cables and presence of bilateral connections) on the trolleygrid energy demand using measured and simulated bus traction, heating, and velocity profiles

II. THE FULL TROLLEYGRID MODEL

A. The Bus Power Model

The trolleygrid model (figure 6) begins with the creation of bus demand from measured velocity and power cycles, and randomized traffic and stoplight probability data.

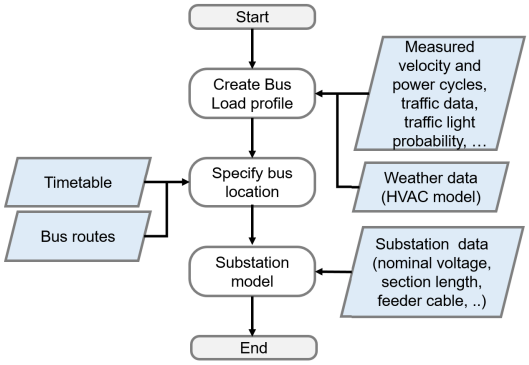

Fig. 6. Flowchart of the trolleybus grid model.

The bus powers are given by Eq.1. During braking, the bus power, P_{bus}, is the auxiliaries power P_{aux} plus the net exchanged with the grid P_{net}, and the excess power P_{BR} that is wasted in the braking resistors (see figure 7 and Eq.1). While in traction mode, the bus power is simply the traction P_{tr} and the auxiliaries demand, P_{aux}.

$$P_{\text{bus},j} = \begin{cases} P_{\text{net},j} + P_{\text{aux},j} + P_{\text{BR},j} & \text{if braking} \\ P_{\text{tr},j} + P_{\text{aux},j} & \text{if traction} \end{cases} j = 1..N_{\text{bus}} \quad (1)$$

The auxiliaries are -predominately- the HVAC load plus other base loads such as the on-board lights, screens, door motors, the control systems, etc.:

$$P_{\text{aux}} = P_{\text{HVAC}} + P_{\text{base}} \quad (2)$$

The HVAC requirement is calculated by a thermodynamic heat exchange model between the trolleybus and the surrounding environment and contains the following components:

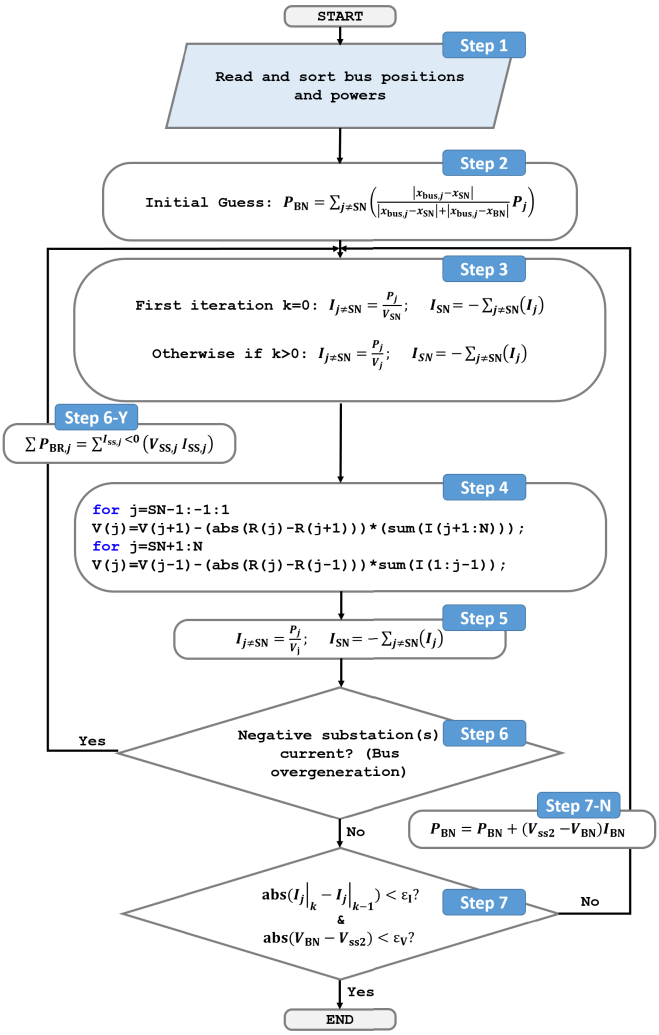

Fig. 7. Flowchart of the grid model logic.

- Q_c: Conductive and convective heat transfer load
  The heat exchange through the vehicle body due to the difference in temperature between the cabin and the external environment.
- Q_v: Ventilation heat
  The heat exchange due to the forced air ventilation and air circulation (air quality requirement). This heat component is determined by the inside-outside temperature difference and by the difference in humidity.
- Q_d: Door-opening air ventilation
  The air ventilation due to the opening of the doors for passenger transit. This heat component is determined by the inside-outside temperature difference and by the difference in humidity.
- Q_s: Solar heat load
  The solar heat gain due to solar radiation: direct, diffuse and reflected radiation.
- Q_m: Metabolic heat load
  The metabolic heat gain from the passenger bodies. This heat component depends on the number of passengers and on the characteristics of the passengers and their standing/seating status. The number of passengers was assumed to be constant in the Arnhem simulations, but the model can be extended with passenger traffic estimations (e.g., [38], [39]).

For the Arnhem bus types, the HVAC system is controlled with a duty cycle (t_{cycle}) of 300 seconds, or 5 minutes. The on-time, t_{on}, of the HVAC system for each period is dictated by the average HVAC power requirement of the bus during that cycle:

$$t_{on} = t_{cycle} \frac{\overline{P_{HVAC}}}{P_{rated}} \tag{3}$$

where $\overline{P_{HVAC}}$ is the average power requirement in the 5 minutes and P_{rated} is the nominal HVAC power, namely 36.5 kW for the Arnhem system. Finally, P_{base} is taken as 5 kW. Once the bus power is computed, the location of the bus is obtained from the local timetables and bus routes. The load demands and the positions of the buses are an input to the grid model.

B. The Grid Model

The grid model is based on the backward-forward sweep method [40]. A flowchart of the full model is presented in figure 7. The substation is taken as a slack node (Slack Node (SN)), with a fixed nominal voltage at the rectifier output (i.e., before the feeder cable voltage drop) that delivers the total power demand on the supply zone (bus loads minus the regenerating bus exchanges).

When two sections are connected bilaterally, however, there are two slack nodes, adding complexity to the model in estimating the power delivered by each substation (the load share of each substation). If there is one bus on the supply zone, and the two substations are at the same nominal voltage, then the power share ratio of each substation is trivially the ratio of the impedances between each substation and the bus. However, this is generally not the case as there are multiple buses on the section, and the two substations have different nominal voltages. The solution requires then an iterative process. An original method suggested in this paper (steps 2, 7, and 7-N in figure 7) allows the same unilateral model to be extended for this bilateral case by modelling the second substation (the bilateral node, BN) as a trolleybus in regenerative braking mode with a variable power, P_{BN}. At each iteration, the power of this virtual bus node is updated until its voltage V_{BN} converges to the known voltage of the bilateral substation, V_{ss2}.

The algorithm is described in figure 7 and procedes as follows:

- *Step 1*: The model starts by reading and sorting the positions and powers of all the nodes on the supply zone
- *Step 2*: An initial guess is then made for P_{BN} by an impedance-weighted sum of the bus nodes on the supply zone
- *Step 3*: At the first iteration step, the voltage at each node is assumed to be the voltage of the SN, and therefore the current at each node is the power of the node divided by V_{BN}. At later iterations, with a voltage assigned to each node (from step 4 of the previous iteration), the

current is obtained by dividing the power of each node by its voltage

- *Step 4*: The model starts from SN and sweeps across all nodes. Each node voltage is the voltage of its adjacent node minus the resistive voltage drop between them (see also Eq.4)
- *Step 5*: The algorithm sweeps back across all the nodes and updates their currents. The slack node is then set to deliver the sum of all the node currents
- *Step 6*: As the model is concerned with non-reversible substations, I_{SN} in step 5 is checked if negative (over-sharing of braking energy)
- *Step 6-Y*: If I_{SN} is negative, step 6-Y reduces the power of the generating buses by the amount that is being sent into the substation. In practical terms, this means the buses are wasting this energy on their on-board braking resistors
- *Step 7*: If I_{SN} is not negative, the model checks for convergence and exits if it is achieved. A tolerance is defined for the current at each node (here, 0.2A) and for the voltage of the Bilateral Node (BN) (here, 0.5V)
- *Step 7-N*: If the voltage of the virtual bus at BN is found to be below (or above) V_{ss2}, this means that P_{BN} is lower (or higher, respectively) than it should be, and it is updated

The total impedance between two nodes n and n-1, $R_{n,n-1}$, is obtained from the equivalent impedance model considering the impedance of the supply and return lines and the effect of the parallel connections between them, as explained in the section III-A and III-B.

$$R_{n,n-1} = \rho \cdot |x_n - x_{n-1}| \tag{4}$$

$$V_{\mathrm{c},n} = \begin{cases} V_{\mathrm{s},n} - R_{\mathrm{f},n} \cdot i_{\mathrm{s},n} & i_{\mathrm{s},n} > 0 \\ V_{\mathrm{s},n} + V_{\mathrm{ds},n} & i_{\mathrm{s},n} = 0 n = \mathrm{SN},\ \mathrm{BN} \end{cases} \tag{5}$$

It is important to note that the voltage at the connection point of each substation to the section, V_{c}, is given by Eq.5. If the substation is supplying power, this voltage is equal to the substation voltage, V_{s}, minus the voltage drop across the feeder cable resistance R_{f}. If the substation is not supplying power, the voltage is equal to the substation nominal voltage plus any voltage blocked by the rectifier diodes, V_{ds}.

The model was verified by comparing its yearly energy output to the yearly measured demand of the grid in 2019. The error, calculated by Eq.6, was 3.8%. This equation is used to calculate the percentage errors throughout this paper.

$$\mathrm{Error} = \frac{\mathrm{Value} - \mathrm{Simulated/Estimated\ Value}}{\mathrm{Value}} \cdot 100[\%] \tag{6}$$

III. The Study of the Model Elements

A. The Overhead Lines Impedance

This subsection looks into the error caused by ignoring the inductive component of the overhead line impedance.

The impedance of the overhead lines that provide power to the trolleybuses is largely modelled as purely resistive. Few papers look into a resistive-inductive line, especially when matters of system stability or control are studied as

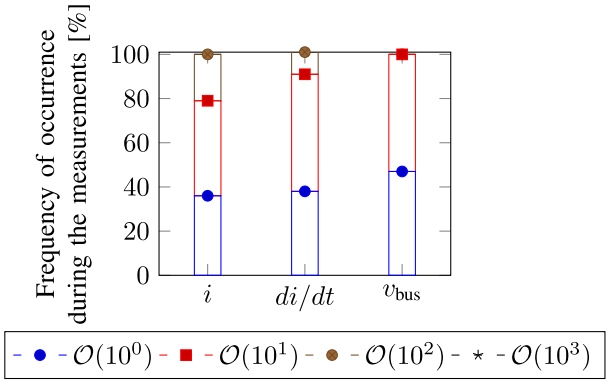

Fig. 8. Analysis of the trolleybus measurement data across the different Arnhem bus lines for the estimation in Eq.10. The order of magnitude of the current i and its derivative di/dt is consistently at or below $\mathcal{O}(10^2)$. The bus velocity, v_{bus},is always at or below $\mathcal{O}(10^1)$.

the capacitance of the added converters forces a study of the dynamic conditions [17].

The voltage drop across the overhead feeding (or return) line, ΔV_{fd}, is due to its resistance and inductance. As the bus is in motion, the drop across one line (feeding or return) can be written as:

$$\Delta V_{\mathrm{fd}} = \frac{d(Li)}{dt} + Ri \tag{7}$$

$$\Delta V_{\mathrm{fd}} = \lambda x_{\mathrm{bus}} \frac{di}{dt} + \frac{d(\lambda x_{\mathrm{bus}})}{dt} i + \rho x_{\mathrm{bus}} i \tag{8}$$

$$\Delta V_{\mathrm{fd}} = \lambda x_{\mathrm{bus}} \frac{di}{dt} + v_{\mathrm{bus}} \lambda i + \rho x_{\mathrm{bus}} i \tag{9}$$

where λ is the inductance per meter (H/m) of the transmission lines (order of 10^{-7} [41]), x_{bus} is the bus distance from the substation in m, v_{bus} is the bus velocity in m/s, ρ is the resistance per m (Ω/m) of the transmission lines (order of 10^{-4}), and i is the current drawn by the bus.

The measured bus current and its derivative in Arnhem (figure 8) shows that they are consistently at the order of 10^2 or below. The measurements also show that the bus velocity, v_{bus}, is always at or below values of the order of $\mathcal{O}(10^1)$.

Consequently,

$$\begin{aligned} \mathcal{O}(\Delta V_{\mathrm{fd}}) &= \mathcal{O}(10^{-7}) \cdot \mathcal{O}(10^3) \cdot \mathcal{O}(10^2) \\ &\quad + \mathcal{O}(10^1) \cdot \mathcal{O}(10^{-7}) \cdot \mathcal{O}(10^2) \\ &\quad + \mathcal{O}(10^{-4}) \cdot \mathcal{O}(10^3) \cdot \mathcal{O}(10^2) \\ &= \mathcal{O}(10^{-2}) + \mathcal{O}(10^{-4}) + \mathcal{O}(10^1) \end{aligned} \tag{10}$$

As the bus voltage itself is at the order of $\mathcal{O}(10^2)$, Eq.10 shows that the assumption of neglecting the line inductance (first two terms of Eq.9) is a valid one for the calculation of the voltage drop across the overhead line. In other terms:

$$\therefore \Delta V_{\mathrm{fd}} \approx Ri \quad \text{(feed or return line)} \tag{11}$$

The conclusion is to model the line impedance as resistive in a steady-state model, offering the possibility of a simpler simulator without any significant error in the output. An inductance component is, however, needed in any dynamic model that looks, for example, at the stability of the grid after the addition of the PV and/or EV chargers and/or storage especially as the

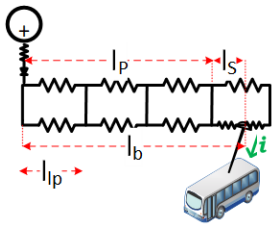

Fig. 9. Circuit representation and nomenclature of the parallel lines connection between (here shown) two feed/positive overhead lines. For simplicity, the return overhead lines (also paralleled) are omitted from the figure.

added converters will introduce a significant capacitance to be seen by the substation and the line inductance.

B. The Overhead Parallel Lines

This section looks into the error caused by different approximation methods of the overhead line total impedance.

The parallel lines, as introduced earlier, contribute to a lower equivalent impedance in the circuit.

The total voltage drop between the substation and the bus can be given by the expression:

$$\Delta V_{\text{tr}} = 2 \cdot (\frac{\rho}{2} l_{\text{p}} + \rho l_{\text{s}} (1 - \frac{l_{\text{s}}}{2 l_{\text{lp}}})) i \tag{12}$$

where the term '2' accounts for lumping the feeder and the return lines, and figure 9 shows the other key parameters. The parallel lines are separated (on average) by a distance of l_{lp}. The bus distance from the substation, l_{b}, is composed of a fully paralleled distance, l_{p}, that is the highest integer multiple of l_{lp} lower than or equal to l_{b}, and a single distance l_{s}.

This equation requires precise knowledge of the parallel lines position, and the distance in between them. This information is not readily available as the ultimate position of the parallel lines is subject to changes between the design stage and the actual implementation by the contractors. The voltage drop can either be approximated by ignoring the current path division in the last single section, and assuming that all the current passes through the shortest path to the bus after l_{p}, the highest integer multiple of the parallel lines (Approximation 1):

$$\Delta V_{\text{tr}} = 2 \cdot (\frac{\rho}{2} l_{\text{p}} + \rho l_{\text{s}}) i \tag{13}$$

or by lumping the total resistance, R, as an equivalent parallel resistance of R/2 (Approximation 2):

$$\Delta V_{\text{tr}} = 2 \cdot (\frac{\rho}{2} l_{\text{b}}) i \tag{14}$$

Figure 10 shows the total voltage drop between the substation (700V nominal, 100 mm^2 Cu lines) and the bus as a function of the bus power and distance. The current is obtained iteratively from the bus power by:

$$i = \frac{P_{\text{bus}}}{V_{\text{bus}}} = \frac{P_{\text{bus}}}{V_{\text{s}} - \Delta V_{\text{tr}}} \tag{15}$$

As expected, Approximation 1 overestimates the voltage drops (up to 40V) while Approximation 2 underestimates them (within 10V). However, the former introduces more serious

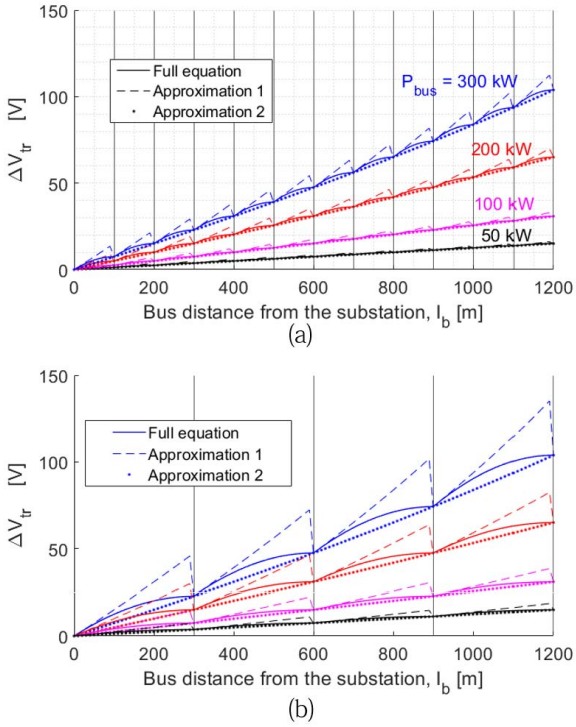

Fig. 10. The voltage drop between the substation and the bus as a function of the bus power (P_{bus}) and distance from the substation (l_{b}) The parallel lines in (a) are at every 100m and in (b) at 300m, and shown with vertical lines. Approximation 1 always overestimates the voltage drop (up to 40V), while Approximation 2 always underestimates it (but errors under 10V).

errors, especially when the bus is getting close to the end of a parallel connection. This is because as the bus comes closer to the parallel connection, Approximation 1 counts it as a full impedance, while it is in reality nearing an equivalent half-impedance. Approximation 2 is also an attractive solution as it does not require knowledge of the location of the parallel connections or the spacing between them.

C. The Bus Auxiliaries Power

This section looks into the error caused by ignoring the Heating, Ventilation, and Air Conditioning (HVAC) power demand of the trolleybuses.

Recent measurements in Arnhem have revealed that the bus auxiliaries demand, mainly the HVAC, are as significant as its traction load demand [31]. This order of magnitude is in line with previous values reported in literature [30].

This motivates the inclusion of HVAC in the study of a trolleygrid as is done in [6], [14]. It is worth noting, however, that the different climate conditions and thermal comfort standards between trolley cities require a location-specific HVAC load to be simulated, rather than the addition of a constant load.

Figure 11 shows the Arnhem total supplied energy measurements at the substations for the January and May months of 2016 till 2019.

January and May run the same schedule in Arnhem, but differ only in the ambient temperature (2-4 degrees and 13-18 degrees Celsius, respectively). This translates into a

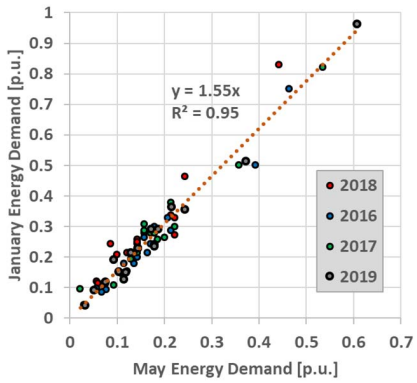

Fig. 11. Per-unit measurements of the January and May energy demand for the Arnhem substations over 4 years (normalized for data sensitivity concerns).

TABLE II
CHARACTERISTICS OF THE 6 DAYS OF THE YEAR (OUT OF 365) CHOSEN FOR THE GRID CASE STUDY IN THIS PAPER REPRESENTING DIFFERENT TRAFFIC AND AUXILIARIES CONDITIONS IN THE ARNHEM TROLLEYGRID

Day	Schedule Category	Traffic	Auxiliaries (HVAC)
1	School holiday week	High	High (winter)
117	Sunday & special holiday	Low	Low (spring)
197	Summer weekday	Low	Medium (summer)
200	Summer Saturday	Low	Medium (summer)
268	Regular weekday	High	High (winter)
305	Regular Saturday	Low	High (winter)

heavy HVAC heating demand in January, while the May weather does not trigger as much heating or air conditioning.

The measurements show that while the HVAC is expected to effectively double the demand of the substation, the actual substation load increases only by about 55%. This reflects the effective use of the regenerative braking and the importance of modelling these two components together for an accurate model of the trolleygrid.

D. The Bus Regenerative Braking

This section looks into the error caused by ignoring the regenerative power of trolleybuses. For the remaining case studies, six exemplary days (Table II) are chosen to highlight the key operating modes of the Arnhem trolleygrid. The days were chosen to also represent different HVAC demands throughout the year.

The bilaterally connected sections Z and W in Arnhem (figure 12) are simulated with and without regenerative braking by removing the negative power from the created bus load (before adding the HVAC). The results are summarized in Table III. Errors as high as 34.4% can be expected in the power calculations in high traffic/high HVAC sceanrios (Days 1 and 268) between the actual scenario (with) and the assumption (without) as per Eq.6. This is expected as the regenerative braking on those days is efficiently recuperated

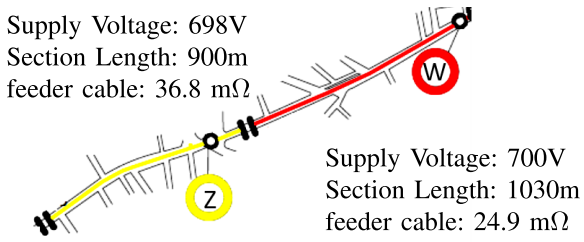

Fig. 12. Regenerative braking: Layout of the investigated sections Z and W in Arnhem and their parameters.

TABLE III
DAILY ENERGY DEMAND FOR SECTIONS Z AND W IN ARNHEM WHEN SIMULATED WITH AND WITHOUT (W/O) CONSIDERING REGENERATIVE BRAKING

	Substation Z [kWh]			Substation W [kWh]		
Day	with	w/o	Error%	with	w/o	Error
1	270	298	10.4 %	262	352	34.4 %
117	130	138	6.2 %	122	138	13.1 %
197	272	286	5.1 %	171	181	5.8 %
200	241	254	5.4 %	163	172	5.5 %
268	328	357	8.8 %	290	340	17.2 %
305	321	347	8.1 %	255	283	11.0 %

by the HVAC and neighboring buses, while it is in this new case being supplied by the substations. In low traffic scenarios (Day 200), the error is still above 5%.

E. The Section Feeder Cables

This section looks into the error caused by ignoring the section feeder cable. First a case study is presented, then a method to approximate when the feeder cable can indeed be ignored without significant errors.

1) The Feeder Cable Case Study: As explained earlier, the section feeder cables are lines that connect the substations to the sections that they supply. These lines are thicker than the overhead lines on the sections as they need to carry the current to multiple sections. The consequence of this is that the feeder cables have lower resistance than that of the overhead line and tend to be ignored in trolleybus simulations. Parallel line connections, however, effectively halve the impedance of the overhead lines, making the feeder cables a modelling necessity, especially when they are long. In Arnhem, for example, some feeder cables go beyond 1 kilometer in length. In dense urban environments, it is expected than feeder cables can be of such lengths as there is no space in city centers for bulky rectifier stations. To highlight the effect of including the feeder cables, a feasibility study is performed on a substation in Arnhem on the introduction of 100kW In-Motion-Charging (IMC) buses. The IMC battery is modelled by adding 100 kW to the bus load before running the grid model, i.e., in the "Create Bus Load Profile" step in the flowchart of figure 6. This method

TABLE IV

EXAMPLE OF A STUDY RESULTING IN FALSE RESULTS BY IGNORING THE FEEDER CABLE ON A SAMPLE SECTION IN ARNHEM DURING A SUMMER SATURDAY SCHEDULE (DAY 200)

Minimum line voltage during the day			
Present case: No IMC operation		Study: With 100kW IMC buses	
Feeder: Yes	Feeder: No	Feeder: Yes	Feeder: No
520V	569V	396V	514V

assumes that the IMC battery is never at the maximum battery SOC while under the section, and therefore is always charging.

The studied section has the following parameters: substation nominal voltage of 698V, 630 mm^2 Cu feeder cables of 1000 meters. Table IV summarizes the results of the study. Ignoring the feeder cable gives the green light to the introduction of IMC buses with a minimum line voltage well above the 400V operational limit of the buses. On the other hand, including the feeder cable shows the voltage dipping below the minimum grid operational threshold, which would cause the bus to shut off, and disturb the daily operation.

2) Estimating the Expected Error: The effect of the section feeder cable, however, is a function of its length and the power that it delivers. Short lines and/or low traffic sections can still have their feeder cables ignored. The below set of equations offer an estimation of the error incurred. For a substation seeing a total energy demand ΣP_s, the total power demand can be approximated as:

$$P_{\text{s, tot}} = \alpha \Sigma P_{\text{s}} \tag{16}$$

where the factor α accounts for the average losses on that section (e.g., for 6% transmission losses, $\alpha = 1.06$). The current supplied from the substation, I_{s}, can be written from Eq.16 in terms of the substation voltage V_{s} as:

$$I_{\text{s}} = \alpha \frac{\Sigma P_{\text{s}}}{V_{\text{s}}}, \tag{17}$$

allowing the losses in the feeder cable (of resistance R_{f}) to be calculated by:

$$P_{\text{loss, f}} = R_{\text{f}} (\alpha \frac{\Sigma P_{\text{s}}}{V_{\text{s}}})^2, \tag{18}$$

Finally, the portion of the power lost in the feeder cable to the total power in the section can be approximated from Eq.18 by:

$$\frac{P_{\text{loss, f}}}{\Sigma P_{\text{s}}} = R_{\text{f}} \alpha^2 \frac{\Sigma P_{\text{s}}}{V_{\text{s}}^2}, \tag{19}$$

Using 17, the voltage drop in the feeder cable can also be estimated by:

$$\Delta V_{\text{f}} = R_{\text{f}} \alpha \frac{\Sigma P_{\text{s}}}{V_{\text{s}}}. \tag{20}$$

To highlight the significance of these equations, figures 13 and 14 show the expected errors as a function of the substation feeder cable length and the power delivered. Typical values from the Arnhem grid are shown also on the figure. The error is defined between the actual case (with feeder cable) and the assumption made not to model the feeder cable. Some substations would see less than 1% error in the power calculations and less than 5V in the voltage calculations if the section feeder cables are ignored. However, some see more than 5% error and 30V in the power and the voltage computations, respectively. This proves the idea that the feeder cable assumption can be made case-by-case.

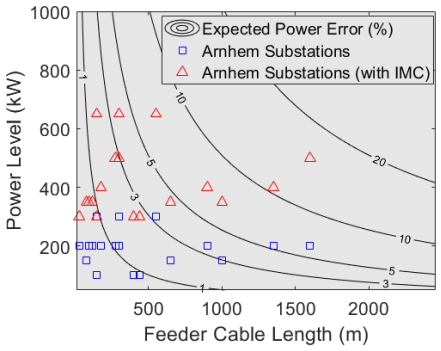

Fig. 13. Error expected in the power calculation (Eq.19)as a function of the feeder cable length and section power level when the section feeder cable is ignored. Values of Arnhem substations with and without IMC are marked.

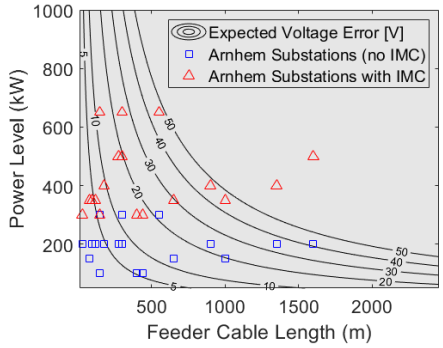

Fig. 14. Error expected in the voltage calculation (Eq.20)as a function of the feeder cable length and section power level when the section feeder cable is ignored. Values of Arnhem substations with and without IMC are marked.

Important to notice as well how IMC substations see greater errors. This shows again that while the current trolleygrids can be sometimes modelled with certain assumptions, the trolleygrid of the future requires more sophisticated models such as the one presented in this paper.

F. The Bilateral Connections

This section looks into the error caused by not considering bilateral connections in a trolleygrid.

A straightforward (and computationally light) option is be to model two bilaterally connected section as isolated, unilateral sections. Measurements and simulations [7], [25], however, indicate that this assumption would not be valid as there could be significant errors in the voltage and power levels.

As a case study, figure 15 shows the two bilaterally connected sections X and Y in Arnhem. Tables V and VI show the expected error in simulating X and Y as bilateral or unilateral sections. While the errors in the sum of the loading of the two sections are mostly insignificant, the individual loading of each substation sees errors as high as 25%. Under-loading of the

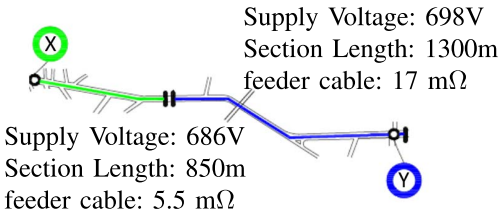

Fig. 15. Bilateral Connection: Layout of the investigated sections X and Y in Arnhem and their parameters.

TABLE V

DAILY ENERGY DEMAND FOR SUBSTATIONS X AND Y IN ARNHEM WHEN SIMULATED WITH THE ASSUMPTION OF BEING UNILATERAL (UNI), AND WHEN CORRECTLY MODELLED AS BILATERAL (BI) SUBSTATIONS

	Substation X [kWh]			Substation Y [kWh]			Sum X & Y [kWh]		
Day	Uni	Bi	Error%	Uni	Bi	Error%	Uni	Bi	Error%
1	164	146	12%	347	359	-3.3%	511	505	1.2 %
117	71	64	11%	155	149	4.0%	226	213	6.1 %
197	95	86	11%	147	157	-6.4%	242	243	-0.4%
200	96	83	16%	141	151	-6.6%	237	235	0.9 %
268	195	156	25%	237	272	-13%	432	428	0.9 %
305	146	126	16%	228	244	-6.6%	374	369	1.4 %

TABLE VI

MINIMUM LINE VOLTAGE IN A DAY FOR SUBSTATIONS X AND Y IN ARNHEM WHEN SIMULATED WITH THE ASSUMPTION OF BEING UNILATERAL (UNI), AND WHEN CORRECTLY MODELLED AS BILATERAL (BI) SUBSTATIONS

	Substation X (686V)			Substation Y (698V)		
Day	Uni [V]	Bi [V]	Error [V]	Uni [V]	Bi [V]	Error [V]
1	627	646	19	607	646	39
117	645	642	-3	599	642	43
197	627	648	21	598	648	50
200	627	648	21	569	648	79
268	652	642	-10	603	642	39
305	617	622	5	490	622	132

station (as far as -13%) is also reported. Additionally, the voltage drops can be as far as 132V. The bilaterally connected sections do not see a voltage below 622V, while the unilateral sections sometimes dip into the range of 500 and 400V. This could lead to large errors in the design and control of, for example, EV chargers and storage control algorithms on a particular section.

G. The Substation Voltage

This section looks into the error of assuming a theoretical value for the substation voltage (commonly 700V) instead of using the actual substation nominal voltage.

Running sections X and Y as unilateral sections with their actual voltage versus 700V did not produce significant errors

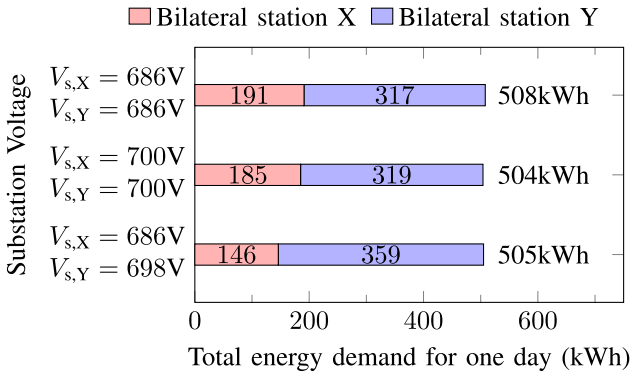

Fig. 16. The different total energy supply by two bilaterally connected sections (X and Y) in Arnhem for different substation voltages for the same one-day load (Day 1).

(less than 1kWh per day from the values reported in Table V). However, figure 16 shows an interesting behavior when the energy demand for substations X and Y is simulated with their nominal voltages or with the common 700V assumption. It can be observed that while the sum of the daily energy supplied by the two substations has an error of only a few kWh, the individual energy share of the load by the substations is shifted. This means that the nominal voltages of the bilateral substations play a role in the power sharing between them. Therefore, any study of the individual demand of a bilaterally-connected substation requires an accurate input of the substation voltages, otherwise it could lead to large errors in the design and control of EV chargers and storage control algorithms, for example.

IV. CONCLUSION

This paper proposed a comprehensive model for a trolleybus grid, including six elements that are often ignored in literature (points B to G below.) Another point, point A, was found to be indeed negligible. To quantify the influence of these elements on the modelling of the grid, case studies were conducted using a verified simulation model, as well as four years of substation energy measurements and over 70 hours of trolleybus measurements in the trolleygrid of Arnhem, The Netherlands. The results are summarized below:

- III-A) The overhead wire impedance: The impedance can be assumed as purely resistive for a steady state model. The inductive component of the lines causes a voltage drop at the order of 10^{-2} for a bus, while the resistive drop is at the order of 10^{1}.
- III-B) The parallel lines: The impedance seen between two nodes can be assumed as half the impedance of the line connecting them.
- III-C) The bus auxiliaries load: The auxiliaries have to be included in the modelling of the trolleybus load, otherwise an average error of 55% is expected in the substation demand calculations.
- III-D) Regenerative braking: The regenerative braking must be included in a trolleygrid model. Errors as high as 34% in the energy demand have been reported, otherwise.

- III-E) The section feeder cable: This line has to be included in a trolleygrid model, depending on its length and the power it typically carries. A set of equations is presented in this paper to make the judgement.
- III-F) Bilateral connection: The modelling of two bilaterally connected sections as two isolated, unilateral sections is not recommended, except for total grid consumption calculations. The loading of individual substations and line voltages included serious errors (maximum of 25% and 132V, respectively).
- III-G) Substation nominal voltage: The exact substation voltage is crucial when modelling bilaterally connected substation as it alters the load share of each substation. For unilateral substations, the difference is not significant.

In conclusion, as the trolleygrid is expanding and adapting to the advancements in smart grid technologies and energy savings, any future research into trolleygrids, especially on the line voltage and power levels (for integration of PV or IMC, for example,) needs to consider the full specifics of the trolleygrid as mentioned in this paper.

ACKNOWLEDGMENT

The authors would also like to thank Hans Aldenkamp and Niek Limburg from Connexxion, Arnhem, for their valuable input and data.

REFERENCES

[1] L. Brunton, "The trolleybus story," *IEE Rev.*, vol. 38, no. 2, pp. 57–61, Feb. 1992.

[2] D. Perrotta, B. Ribeiro, R. J. F. Rossetti, and J. L. Afonso, "On the potential of regenerative braking of electric buses as a function of their itinerary," *Proc.-Social Behav. Sci.*, vol. 54, pp. 1156–1167, Oct. 2012.

[3] S. Hamacek, M. Bartłomiejczyk, R. Hrbáč, S. Mišák, and V. Stýskala, "Energy recovery effectiveness in trolleybus transport," *Electr. Power Syst. Res.*, vol. 112, pp. 1–11, Jul. 2014.

[4] D. Iannuzzi, D. Lauria, and P. Tricoli, "Optimal design of stationary supercapacitors storage devices for light electrical transportation systems," *Optim. Eng.*, vol. 13, no. 4, pp. 689–704, 2011.

[5] D. Iannuzzi, F. Ciccarelli, and D. Lauria, "Stationary ultracapacitors storage device for improving energy saving and voltage profile of light transportation networks," *Transp. Res. C, Emerg. Technol.*, vol. 21, no. 1, pp. 321–337, 2012.

[6] B. Destraz, P. Barrade, A. Rufer, and M. Klohr, "Study and simulation of the energy balance of an urban transportation network," in *Proc. Eur. Conf. Power Electron. Appl.*, Sep. 2007, pp. 1–10.

[7] M. Z. Chymera, A. C. Renfrew, M. Barnes, and J. Holden, "Modeling electrified transit systems," *IEEE Trans. Veh. Technol.*, vol. 59, no. 6, pp. 2748–2756, Jul. 2010.

[8] A. Finlayson, C. J. Goodman, and R. D. White, "Investigation into the computational techniques of power system modelling for a DC railway," in *Proc. WIT Trans. Built Environ.*, vol. 88, Jun. 2006, pp. 123–133.

[9] D. Iannuzzi and P. Tricoli, "Speed-based state-of-charge tracking control for metro trains with onboard supercapacitors," *IEEE Trans. Power Electron.*, vol. 27, no. 4, pp. 2129–2140, Apr. 2012.

[10] D. Cornic, "Efficient recovery of braking energy through a reversible DC substation," in *Proc. Electr. Syst. Aircr., Railway Ship Propuls.*, Oct. 2010, pp. 1–9.

[11] Y. Warin, R. Lanselle, and M. Thiounn, "Active substation," in *Proc. World Congr. Railway Res. (WCRR)*, Lille, France, May 2011.

[12] G. Stana and V. Brazis, "Trolleybus motion simulation by dealing with overhead DC network energy transmission losses," in *Proc. 18th Int. Sci. Conf. Electric Power Eng. (EPE)*, May 2017, pp. 1–6.

[13] J. J. Mwambeleko, T. Kulworawanichpong, and K. A. Greyson, "Tram and trolleybus net traction energy consumption comparison," in *Proc. 18th Int. Conf. Electr. Mach. Syst. (ICEMS)*, Oct. 2015, pp. 2164–2169.

[14] M. Bartłomiejczyk and M. Połom, "Multiaspect measurement analysis of breaking energy recovery," *Energy Convers. Manage.*, vol. 127, pp. 35–42, Nov. 2016.

[15] M. Salih *et al.*, "Impact assessment of integrating novel battery-trolleybuses, PV units and EV charging stations in a dc trolleybus network," in *Proc. 2nd E-Mobility Power Syst. Integr. Symp.*, 2018, pp. 1–6.

[16] M. Salih *et al.*, "Optimized positioning for storage systems in an LVDC traction grid with non-receptive power sources and photovoltaic systems," in *Proc. 9th Solar Storage Integr. Workshop*, 2019.

[17] A. Rufer, D. Hotellier, and P. Barrade, "A supercapacitor-based energy storage substation for voltage compensation in weak transportation networks," *IEEE Trans. Power Del.*, vol. 19, no. 2, pp. 629–636, Apr. 2004.

[18] E. Sindi, L. Y. Wang, M. Polis, G. Yin, and L. Ding, "Distributed optimal power and voltage management in DC microgrids: Applications to dual-source trolleybus systems," *IEEE IEEE Trans. Transport. Electrific.*, vol. 4, no. 3, pp. 778–788, Sep. 2018.

[19] D. Baumeister *et al.*, "Modelling and simulation of a public transport system with battery-trolleybuses for an efficient e-mobility integration," in *Proc. 1st E-Mobility Power Syst. Integr. Symp.*, Oct. 2017, pp. 1–7.

[20] P. Arboleya, B. Mohamed, and I. El-Sayed, "DC railway simulation including controllable power electronic and energy storage devices," *IEEE Trans. Power Syst.*, vol. 33, no. 5, pp. 5319–5329, Sep. 2018.

[21] M. Wazifehdust *et al.*, "Potential analysis for the integration of renewables and EV charging stations within a novel LVDC smart-trolleybus grid," in *Proc. 25th Int. Conf. Electr. Distrib. (CIRED)*, Madrid, Spain, Jun. 2019, Paper 1505.

[22] D. Zhang, J. Jiang, L. Y. Wang, and W. Zhang, "Robust and scalable management of power networks in dual-source trolleybus systems: A consensus control framework," *IEEE Trans. Intell. Transp. Syst.*, vol. 17, no. 4, pp. 1029–1038, Apr. 2016.

[23] G. Stana and V. Brazis, "Mathematical calculation of power transmission related parameters in simulations of overhead grid-connected electric public transport motion," in *Proc. IEEE 61th Int. Sci. Conf. Power Electr. Eng. Riga Tech. Univ. (RTUCON)*, Nov. 2020, pp. 1–6.

[24] G. Stana and V. Brazis, "Trolleybus with ESS motion simulation considering common mass increase and transmission losses," in *Proc. IEEE 58th Int. Sci. Conf. Power Electr. Eng. Riga Tech. Univ. (RTUCON)*, Oct. 2017, pp. 1–6.

[25] M. Bartlomiejczyk, "Modern technologies in energy demand reducing of public transport—Practical applications," in *Proc. Zooming Innov. Consum. Electron. Int. Conf. (ZINC)*, May 2017, pp. 64–69.

[26] B.-Y. Ku and J.-S. Liu, "Solution of DC power flow for nongrounded traction systems using chain-rule reduction of ladder circuit Jacobian matrices," in *Proc. ASME/IEEE Joint Railroad Conf.*, Apr. 2002, pp. 123–130.

[27] D. Zhang, L. Y. Wang, J. Jiang, and W. Zhang, "Optimal power management in DC microgrids with applications to dual-source trolleybus systems," *IEEE Trans. Intell. Transp. Syst.*, vol. 19, no. 4, pp. 1188–1197, Apr. 2018.

[28] Kruch. (2021). *KRUCH Railway Innovations GmbH & Co. KG*. Accessed: Jun. 16, 2021. [Online]. Available: http://kruch.com/

[29] J. Macedo and R. J. Rossetti, "Rush hour traffic conditions impact in electric bus performance: A case study in Porto," in *Proc. DSIE*, 2017, p. 65.

[30] M. Bartłomiejczyk and R. Kołacz, "The reduction of auxiliaries power demand: The challenge for electromobility in public transportation," *J. Cleaner Prod.*, vol. 252, Apr. 2020, Art. no. 119776.

[31] A. S. Tomar, B. Veenhuizen, L. Buning, and B. Pyman, "Estimation of the size of the battery for hybrid electric trolley busses using backward quasi-static modelling," *Multidisciplinary Digit. Publishing Inst. Proc.*, vol. 2, no. 23, p. 1499, 2018.

[32] A. Shekhar, G. C. R. Mouli, S. Bandyopadhyay, and P. Bauer, "Electric vehicle charging with multi-port converter based integration in DC trolley-bus network," in *Proc. IEEE 19th Int. Power Electron. Motion Control Conf. (PEMC)*, Apr. 2021, pp. 250–255.

[33] W. Wu, Y. Lin, R. Liu, Y. Li, Y. Zhang, and C. Ma, "Online EV charge scheduling based on time-of-use pricing and peak load minimization: Properties and efficient algorithms," *IEEE Trans. Intell. Transp. Syst.*, vol. 23, no. 1, pp. 572–586, Jan. 2022.

[34] M. Bartlomiejczyk, "Practical application of in motion charging: Trolleybuses service on bus lines," in *Proc. 18th Int. Sci. Conf. Electr. Power Eng. (EPE)*, May 2017, pp. 1–6.

[35] M. Wołek, M. Wolański, M. Bartłomiejczyk, O. Wyszomirski, K. Grzelec, and K. Hebel, "Ensuring sustainable development of urban public transport: A case study of the trolleybus system in Gdynia and Sopot (Poland)," *J. Cleaner Prod.*, vol. 279, Jan. 2021, Art. no. 123807.

[36] M. Bartłomiejczyk, "Bilateral power supply of the traction network as a first stage of smart grid technology implementation in electric traction," in *Proc. MATEC Web Conf.*, vol. 180, 2018, pp. 1–6.

[37] M. Bartlomiejczyk, "Use of numerical methods in the analysis of traction energy systems-an overview of the practical examples," in *Proc. 1st Int. Sci. Conf. Intell. Inf. Technol. Ind. (IITI)*. Cham, Switzerland: Springer, 2016, pp. 407–418.
[38] Z. Ma, J. Xing, M. Mesbah, and L. Ferreira, "Predicting short-term bus passenger demand using a pattern hybrid approach," *Transp. Res. C, Emerg. Technol.*, vol. 39, pp. 148–163, Feb. 2014.
[39] R. Liu and S. Sinha, "Modelling urban bus service and passenger reliability," in *Proc. 3rd Int. Symp. Transp. Netw. Rel.*, The Hague, The Netherlands, Jul. 2007.
[40] Z. Wang, F. Chen, and J. Li, "Implementing transformer nodal admittance matrices into backward/forward sweep-based power flow analysis for unbalanced radial distribution systems," *IEEE Trans. Power Syst.*, vol. 19, no. 4, pp. 1831–1836, Nov. 2004.
[41] P. C. Sen, *Principles of Electric Machines and Power Electronics*. Hoboken, NJ, USA: Wiley, 2007.

Ibrahim Diab (Student Member, IEEE) received the bachelor's degree in mechanical engineering from the American University of Beirut in 2012 and the master's degree (Hons.) in sustainable energy technologies (SET) with the ESE Department in 2017. He is currently pursuing the Ph.D. degree with the DC Systems, Energy Conversion and Storage (DCE&S) Group, Department of Electrical Sustainable Energy (ESE), Delft University of Technology, The Netherlands, with a focus on transforming the trolleybus grid into an active, sustainable, and multi-functional transport grid of the future. He worked as a Measurement-While-Drilling Engineer with Schlumberger, Saudi Arabia, until August 2014. In 2015, he received the TU Delft "Delft Research Initiative—Energy" Full Scholarship. After graduating, he started with the DCE&S Group as a full-time Teaching Assistant on courses on AC and DC microgrids, electrical power conversion, and the system integration project. He worked as a Co-Creator and a Manager for the professional certificates online courses with the ESE Department on intelligent electrical power grids and on electrical power conversion.

Alice Saffirio received the bachelor's degree in energy engineering from the Politecnico di Milano, Milan, Italy, in 2017, and the master's degree in sustainable energy technologies from the Electrical Engineering, Mathematics and Computer Science Faculty, TU Delft, Delft, The Netherlands, in June 2021. She developed her final master thesis project with the DC Systems, Energy Conversion and Storage (DCE&S) Group, Electrical Sustainable Energy Department on "investigation of the potential of pv in trolleygrids: study of the effect of key performance indicators on the integration of photovoltaic (PV) systems in Trolleygrids–Arnhem and Gdynia case studies." Since September 2021, she has been participating in the International Trainee Program, Statkraft, which involves three job rotations in different roles and in different offices of the company. She first worked as a Wind Project Developer in Milan. She is currently a part of the Power Market Analysis Team in Oslo, Norway. She is still collaborating with the DCE&S Group on publications on the transformation of the trolleygrid into a sustainable transport grid of the future.

Gautham Ram Chandra Mouli (Member, IEEE) received the bachelor's degree in electrical engineering from the National Institute of Technology Trichy, India, in 2011, the master's degree in electrical engineering from the Delft University of Technology, The Netherlands, in 2013, and the Ph.D. degree from Delft University in 2018, for the development of a solar powered V2G electric vehicle charger compatible with CHAdeMO, CCS/COMBO, and designed smart charging algorithms (with PRE, ABB, and UT Austin). From 2017 to 2019, he was a Post-Doctoral Researcher at TU Delft, where his research is focused on power converters for EV charging, smart charging of EVs, and trolley busses. He is the Coordinator and a Lecturer of Massive Open Online Course (MOOC) on electric cars on edX.org with 175,000 learners from 175 countries. He is currently an Assistant Professor with the DC Systems, Energy Conversion and Storage Group, Department of Electrical Sustainable Energy, Delft University of Technology. He is involved in many projects with industrial and academic partners at national and EU level concerning electric mobility and renewable energy, such as PV charging of electric vehicles, OSCD, Trolley 2.0, Flexgrid, Flexinet, and NEON. His current research interests include electric vehicles and charging, PV systems, power electronics, and intelligent control. His project was awarded the "Most significant innovation in electric vehicles" award from IDtechEx in 2018 and the "Best Tech Idea of 2018" by KIJK. He was awarded the Best Paper Prize in the IEEE TRANSACTIONS ON INDUSTRIAL INFORMATICS in 2018, the Best Poster Prize at Erasmus Energy Forum 2016, The Netherlands, and the Best Paper Prize at the IEEE INDICON Conference 2009, India. He is the Vice-Chair of IEEE Industrial Electronic Society Benelux Chapter.

Abhishek Singh Tomar received the B.E. degree in mechanical engineering from Manipal University, India, in 2012, and the M.Sc. degree in automotive systems from the HAN University of Applied Sciences, Arnhem, The Netherlands, in 2015. He is currently a full-time Researcher with HAN Automotive Research, HAN University of Applied Sciences. He works with vehicle and infrastructure data to develop vehicle controls at the tactical and operational level and management strategies for personal and freight mobility optimization. The majority of his research focuses on realizing human-centered data-driven solutions for making automated and electric driving safe, transparent, trustworthy, and acceptable.

Pavol Bauer (Senior Member, IEEE) received the master's degree in electrical engineering from the Technical University of Kosice, Koisce, Slovakia, in 1985, and the Ph.D. degree from the Delft University of Technology, Delft, The Netherlands, in 1995. He is currently a Full Professor with the Department of Electrical Sustainable Energy, Delft University of Technology; the Head of DC Systems, Energy Conversion and Storage Group; a Professor with the Brno University of Technology, Brno, Czechia; and a Honorary Professor with Politehnica University Timişoara, Timişoara, Romania. From 2002 to 2003, he was with KEMA (DNV GL, Arnhem) on different projects related to power electronics applications in power systems. He has authored and coauthored more than 120 journals and 500 conference papers in his field with H factor Google scholar 40, Web of Science 26. He is the author or coauthor of eight books, holds seven international patents, and organized several tutorials at the international conferences. He has worked on many projects for industry concerning wind and wave energy, power electronic applications for power systems, such as smarttrafo, HVDC systems, projects for smart cities, such as PV charging of electric vehicles, PV and storage integration, and contactless charging. He participated in several Leonardo da Vinci, H2020 and Electric Mobility Europe EU projects as a Project Partner (ELINA, INETELE, E-Pragmatic, Micact, Trolley 2.0, OSCD, P2P, and Progressus) and a Coordinator (PEMCWebLab.com-Edipe, SustEner, and Eranet DCMICRO). His main research interests include power electronics for charging of electric vehicles and dc grids. He is the Former Chair of Benelux IEEE Joint Industry Applications Society, Power Electronics and Power Engineering Society Chapter, the Chair of the Power Electronics and Motion Control Council, and a member of the Executive Committee of European Power Electronics Association and the International Steering Committee at numerous conferences.